Enzyme Inhibitors

DOI: 10.1002/ange.200705795

Development of Selective RabGGTase Inhibitors and Crystal Structure of a RabGGTase–Inhibitor Complex**

Zhong Guo, Yao-Wen Wu, Kui-Thong Tan, Robin S. Bon, Ester Guiu-Rozas, Christine Delon, Uyen T. Nguyen, Stefan Wetzel, Sabine Arndt, Roger S. Goody, Wulf Blankenfeldt, Kirill Alexandrov, and Herbert Waldmann**

Rab guanosine triphosphatases (GTPases) constitute the most prominent branch of the Ras superfamily of GTPases and are responsible for a broad range of intracellular trafficking events such as vesicle formation, vesicle and organelle motility, and tethering of vesicles to their target compartments.[1,2] They require the covalent attachment of two geranylgeranyl groups to their C-terminal cysteine residues for biological activity. This modification is catalyzed by Rab geranylgeranyl transferase (RabGGTase, GGTase II) which modifies all 60 mammalian RabGTPases. In contrast to other protein prenyltransferases, such as farnesyltransferase (FTase) and geranylgeranyl transferase I (GGTase I), RabGGTase does not recognize its protein substrate directly but functions in concert with a protein named Rab escort protein (REP).[3] Although numerous effective and specific inhibitors of FTase[4] and GGTase I[5] are known, only one specific but weak phosphonocarboxylate inhibitor of RabGGTase has been reported so far.[6] This is despite the biological importance of RabGGTase and its involvement in the establishment of several diseases. Thus, the aforementioned phosphonocarboxylate was considered to be a lead compound for the development of new treatments for thrombotic disorders and excessive osteoclast-mediated bone resorption, which can cause tumor-induced osteolysis and postmenopausal osteoporosis.[6] More recent studies indicate that inhibition of RabGGTase induces p53-independent apoptosis and additionally validate this enzyme as a promising target for anticancer therapy.[7] According to the findings reported by Ross-Macdonald and co-workers,[7] RabGGTase may be responsible for the proapoptotic activity of the farnesyltransferase inhibitors[4] currently in late-stage clinical trials.[8]

To study the role of RabGGTase in skeletal disorders and cancer and, in general, the biological function of Rab proteins, potent and selective inhibitors of the enzyme with activity in cells would be invaluable. However, such compounds are currently not accessible.[7] Their development would be greatly facilitated by the availability of a crystal structure of RabGGTase in complex with such an inhibitor. However, such a structure is also currently not available. Here we report the identification of such compounds and the first crystal structure of RabGGTase in complex with an inhibitor.

For the development of inhibitors displaying the properties detailed above, we have drawn on our earlier findings that peptides modeled on the naturally occurring FTase inhibitor pepticinnamin E may also inhibit RabGGTase (Scheme 1).[9–11] In order to gain insight into the structural parameters determining inhibition by these tripeptide derivatives, we assembled a library of 469 further peptides and characterized them in an in vitro Rab prenylation assay.

The tripeptide library was synthesized according to methods reported previously (Scheme 1; see also the Supporting Information).[9] Structure variation included different amino acids (for example, Ala, Leu, His, Tyr, Ser, Thr, Lys, Glu, Gln), various long- and short-chain aliphatic, olefinic, or (hetero)aromatic amides at the N terminus, and carboxylic acid, several esters, or various amides at the C terminus; the structural diversity of the collection was thereby guaranteed (see Table 1 for examples).

After release from the solid support, the compounds were purified by HPLC and isolated in analytically pure form (see the Supporting Information for representative HPLC traces). For the evaluation of the tripeptides as RabGGTase inhibitors, we employed a recently developed fluorometric in vitro Rab prenylation assay[11] that monitors the change in fluores-

[*] Dr. K.-T. Tan, Dr. R. S. Bon, Dr. E. Guiu-Rozas, Dipl.-Chem. S. Wetzel, Dr. S. Arndt, Prof. Dr. H. Waldmann
Max-Planck-Institut für molekulare Physiologie
Abt. Chemische Biologie
Otto-Hahn-Strasse 11, 44227 Dortmund (Germany)
and
TU Dortmund, Fachbereich Chemie
44227 Dortmund (Germany)
Fax: (+49) 231-133-2499
E-mail: herbert.waldmann@mpi-dortmund.mpg.de
Z. Guo,[+] Y.-W. Wu,[+] Dr. C. Delon, Dipl.-Chem. U. T. Nguyen, Prof. Dr. R. S. Goody, Dr. W. Blankenfeldt, Dr. K. Alexandrov
Max-Planck-Institut für molekulare Physiologie, Abt. Physikalische Biochemie, Otto-Hahn-Strasse 11, 44227 Dortmund (Germany)
Fax: (+49) 231-133-2399
E-mail: kirill.alexandrov@mpi-dortmund.mpg.de
[+] These authors contributed equally to this work.

[**] RabGGTase: Rab geranylgeranyl transferase. We thank the X-ray communities of the Max-Planck-Institut für molekulare Physiologie (Dortmund, Germany) and the Max-Planck-Institut für medizinische Forschung (Heidelberg, Germany) for collecting diffraction data at the Swiss Light Source of the Paul Scherrer Institute (Villigen, Switzerland) and for giving us generous access and support for the station X10SA. K.A. was supported by a Heisenberg Award of the Deutsche Forschungsgemeinschaft (DFG). This work was supported in part by DFG grants to K.A. (grant no.: AL 484/7-2) and to K.A., R.S.G, and H.W. (grant no.: SFB642), and by the Zentrum für Angewandte Chemische Genomik. R.S.B. thanks the Alexander von Humboldt Stiftung for a scholarship.

Supporting information for this article is available on the WWW under http://www.angewandte.org or from the author.

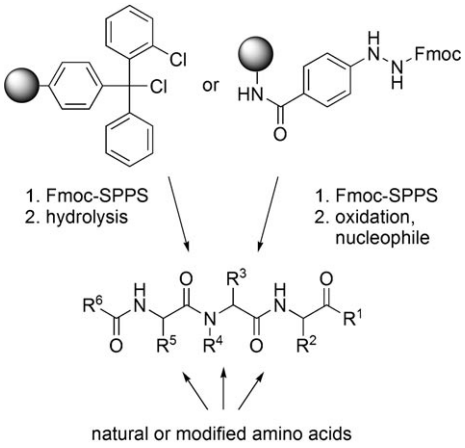

Scheme 1. Solid-phase approach for the synthesis of a library of potential peptide-based RabGGTase inhibitors. Fmoc: 9-fluorenylmethoxycarbonyl; SPPS: solid-phase peptide synthesis.

Table 1: Results of the solid-phase synthesis and inhibition of RabGGTase for a selected group of peptides.

Entry	Cmpd.	R^6–AA1–AA2–AA3–R^1					IC_{50} [μM][a]
		$R^{6[b]}$	AA1	AA2	AA3	$R^{1[b]}$	
1	**1**	Cbz	D-Tyr	Phe	Tyr	OH	4.1 ± 0.3
2	**2**	Cbz	His	(*N*Me)Phe	Tyr	OH	22.7 ± 1.8
3	**3**	Cbz	His	(*N*Me)Phe	Tyr	NHOH	9.0 ± 1.0
4	**4**	Cbz	His	(*N*Me)Phe	Trp	NHOH	5.2 ± 0.7
5	**5**	**I**	His	Phe	Tyr	**A**	2.8 ± 0.4
6	**6**	**II**	His	Phe	Tyr	**A**	4.7 ± 1.0
7	**7**	**II**	Tyr	His	Tyr	**A**	6.3 ± 0.7
8	**8**	**II**	His	His	Tyr	**A**	11.0 ± 1.2
9	**9**	**II**	His	His	Tyr	**B**	5.2 ± 0.8
10	**10**	**II**	Tyr	His	Tyr	**B**	7.2 ± 0.3

[a] All IC_{50} values were determined by at least three independent measurements. [b] Cbz: benzyloxycarbonyl.

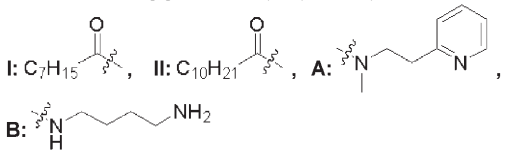

cence of a fluorescent analogue of geranylgeranylpyrophosphate (GGPP) upon transfer to a Rab protein. Briefly, in this analogue, the terminal isoprene unit of the geranylgeranyl group is replaced by a nitrobenzoxadiazole (NBD) fluorophore to yield {3,7,11-trimethyl-12-(7-nitrobenzo-[1,2,5]oxadiazo-4-ylamino)-dodeca-2,6,10-trien-1} pyrophosphate (NBD-FPP; see the Supporting Information for the structure).

During the final step of the catalysis, binding of the NBD-farnesylated C terminus of Rab to REP leads to a dramatic increase in the fluorescence of NBD, thereby providing a convenient readout of the reaction. This assay was adapted for automated screening (for details, see the Supporting Information). After an initial prescreen at a fixed concentration to identify potential inhibitors, the most potent compounds were selected for concentration-dependent inhibition measurements (Table 1). In general, tripeptides rich in histidines and tyrosines, especially as AA1 and AA3, are the best RabGGTase inhibitors. Except for compound **4**, all of the most potent compounds contain a tyrosine residue as AA3. In most of the potent inhibitors, AA2 is an (*N*-methylated)phenylalanine or a histidine. The data indicate that polar C termini like free carboxylic acids (entries 1 and 2), hydroxamic acids (entries 3 and 4), *N*-methyl-*N*-(pyridine-2-yl)ethylamides (entries 5–8), or *N*-aminobutylamides (entries 9 and 10) are beneficial for RabGGTase inhibition. Furthermore, a Cbz group (entries 1–4) or long lipophilic chains (entries 5–10) at the N terminus improve binding to RabGGTase. In general, the introduction of simple alkyl esters at the C terminus, shorter alkyl chains at the N terminus, or small (Gly, Ala), hydrophobic (Val, Leu, Pro), hydrophilic (Ser, Thr, Gln), or charged (Lys, Glu) amino acids leads to a substantial decrease in inhibitory potency (data not shown).

The identified compounds were evaluated for their ability to inhibit all three prenyltransferases in a sodium dodecylsulfate (SDS) PAGE end-point in vitro prenylation assay (Table 2; see also the Supporting Information).[10] These

Table 2: IC_{50} values determined by means of SDS-PAGE end-point assays.

Entry	Inhibitor	RabGGTase IC_{50} [μM]	FTase IC_{50} [μM]	GGTase I IC_{50} [μM]
1	**5**	8.8 ± 0.7	98 ± 4.7	97 ± 31
2	**6**	2.8 ± 0.1	–	> 100
3	**7**	4.3 ± 0.4	–	> 100
4	**8**	10.0 ± 0.9	35 ± 5.8	60 ± 5.3

experiments demonstrated that compounds **5**–**7** are 10–30-fold selective for RabGGTase, while the selectivity of **8** was 3.5–6-fold (see Table 2). In addition, compound **5** is selective for RabGGTase over FTase by a factor of at least 10. Unfortunately, the IC_{50} values of **6** and **7** for FTase were not extractable from the assay. These compounds showed dose-dependent inhibition of FTase, but the inhibition was saturated at less than 50% (see the Supporting Information, Figure S2), which was not observed in the case of the other two prenyltransferases. This finding suggests that these compounds partially inhibit FTase by a mixed competitive and noncompetitive mechanism. Thus, inhibitors **5**–**8** show moderate to fairly good selectivity for RabGGTase over FTase and GGTase I and can be regarded as the first known selective low-micromolar RabGGTase inhibitors.

The IC_{50} values provide an indication of the inhibitory activity of the identified tripeptides under the chosen conditions but do not provide direct information on either their mode of action or their affinity for RabGGTase. Therefore, a series of fluorometric titrations was performed with **8** by using the fluorescence of NBD-FPP bound to RabGGTase as a reporter of the enzyme's interaction with the inhibitor (see the Supporting Information, Figure S3).[10] An example of the results of RabGGTase–NBD-complex titration with **8** is shown in Figure 1. Fitting of the data to the competitive model with 1:1 stoichiometry of the complex led to a K_d value of 1.0 ± 0.08 μM (Figure 1).

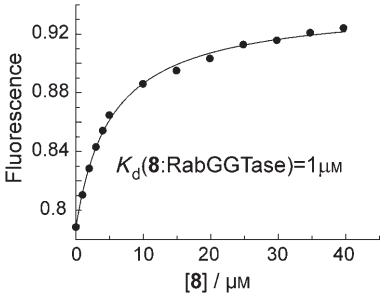

Figure 1. Analysis of the interaction of compound **8** with RabGGTase by using the fluorescence of bound NBD-FPP as a reporter. Titration of NBD-FPP-modified RabGGTase with **8.** The data were fitted by numerical simulation to a competitive model to give a dissociation constant of **8** from RabGGTase of $K_d = (1.0 \pm 0.08)$ μM. (The K_d value for NBD-FPP was fixed at 163 nM). The concentration of NBD-FPP was 400 nM and of RabGGTase was 650 nM (see Figure S3 in the Supporting Information for more experimental details). NBD fluorescence was excited at 479 nm and the data were collected at 547 nm.

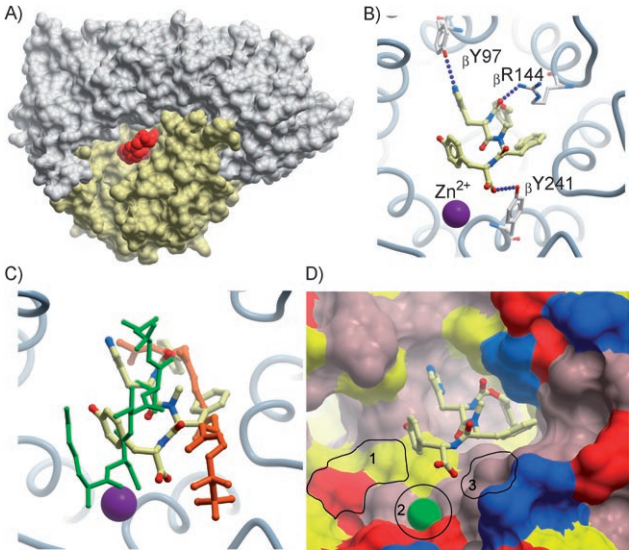

Figure 2. Structural analysis of truncated RabGGTase in complex with **2.** A) Surface representation of RabGGTase. The α and β subunits are shown in gray and yellow, respectively. Compound **2**, shown as a Corey–Pauling–Koltun model in red, binds to the substrate-binding site. B) Interactions of compound **2** with the active site of RabGGTase. The β subunit of RabGGTase is displayed as gray tubes. Compound **2** and interacting side chains of the β subunit are displayed as sticks colored by atom type. Blue dotted lines indicate hydrogen bonds. The Zn^{2+} ion is shown as a purple sphere. C) Superimposition of the structure of RabGGTase in complex with **2** and the structure of GGTase I in complex with substrate peptide KICVIL and a nonhydrolyzable analogue of GGPP (Protein DataBank (PDB) access code: 1N4Q). RabGGTase is displayed as in (B), while the ligands are displayed as ball-and-stick models. The GGTase I substrate peptide is colored green, compound **2** is colored according to atom type, and the GGPP analogue is shown in dark orange. D) Surface representation of the active site of RabGGTase in complex with **2**. Surface residues of the active site are colored as follows: hydrophobic in yellow, polar in pink, positively charged in blue, and negatively charged in red. Highlighted areas represent sites that could be used for additional anchoring of the inhibitor.

In order to gain insight into the molecular details of the interaction between RabGGTase and the identified inhibitors, we used a cocrystallization approach to obtain an enzyme–inhibitor complex structure. After substantial experimentation, crystals of the complex of compound **2** with a truncated version of RabGGTase were obtained and the structure was determined with a resolution of 2.3 Å (Figure 2; for details, see the Supporting Information).

Compound **2** binds in a deep bifurcated cavity containing the active center at the interface of the α and β subunits of RabGGTase (Figure 2A) and adopts an extended conformation with the C terminus pointing outward (Figure 2B). The interaction between RabGGTase and compound **2** is mainly hydrophobic. Only the inhibitor's carbamate group forms a strong hydrogen bond to the protein, namely with the side chain of Arg144 of the β subunit. The imidazole moiety of compound **2** appears to be part of a hydrogen-bonding network involving several water molecules and possibly also Tyr97 of the β subunit. A weak hydrogen bond to Tyr241 in the β subunit anchors the C-terminal carboxylate group of the inhibitor. Superimposition of the structure of the related GGTase I in complex with a monoprenylated peptide and an analogue of geranylgeranyl pyrophosphate (PDB access code: 1N4Q)[12] reveals that the backbone of compound **2** and the histidyl and tyrosyl side chains occupy the protein's substrate-binding site (Figure 2C). The side chain of the C-terminal tyrosine is highly flexible, thereby indicating that it may act as a general gatekeeper to block access of the protein substrate and that its exact nature may not be important. The phenylalanine protrudes into the hydrophobic isoprenoid-binding pocket providing three additional potential anchoring sites for the inhibitor (Figure 2C). Analysis of the complex structure reveals more attachment points in the immediate vicinity of the bound inhibitor that could be employed to improve the affinity and specificity of the inhibitors (Figure 2D). Site 1 is composed of residues Asp287, Pro288, and Phe289, which are located on the tip of helix 12 that ends at the active site. Site 2 is represented by the Zn^{2+} ion and the coordinating His290, while site 3, built of Arg232 and Lys235, is positively charged and, by homology, is expected to anchor the phosphate groups of GGPP. Taken together, these observations open a route to further inhibitor improvement by structure-guided ligand design.

Finally, we wanted to establish whether the identified compounds inhibit Rab prenylation in cellular systems. To this end, COS-7 cells overexpressing an EYFP-Rab7 fusion protein were incubated with the compounds for 24 h and then lysed. The lysate was subjected to in vitro prenylation with recombinant RabGGTase and REP and a biotin-containing analogue of GGPP, biotin–GPP (compound **12**, see the Supporting Information). Prenylated cell lysates were subjected to Western blotting with steptavidin–horseradish peroxidase to detect Rab–geranylbiotin conjugates (Figure 3).

Compounds **2–4** and **6–8** all caused increased labeling of EYFP-Rab7, a result indicating inhibition of prenylation to an extent comparable with that of compactin (which prevents formation of GGPP by inhibiting the mevalonate pathway).

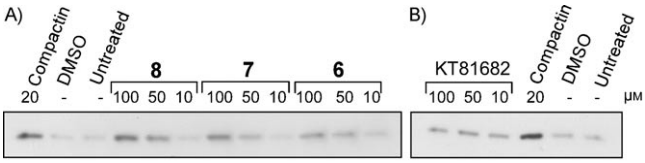

Figure 3. Inhibition of RabGGTase by compounds **6**–**8**. A) COS-7 cells transiently coexpressing EYFP-Rab7 and ECFP-RabGDI were incubated with compounds at the concentrations indicated. Control cells were treated with 20 μM compactin, a known prenylation inhibitor, or with 1% DMSO, or remained untreated. B) Cells treated with KT81682, a compound that is not a RabGGTase inhibitor in cells but displays an in vitro IC_{50} value of (11.6 ± 1.2) μM (not shown) show a signal comparable to the background (DMSO, untreated).

In conclusion, we have developed potent RabGGTase inhibitors selective for this enzyme over FTase and GGTase I and endowed with cellular activity.[13] The availability of these inhibitors may open up new opportunities for the study of RabGGTase and its involvement in the establishment of diseases. In addition, we have determined the first crystal structure of RabGGTase in complex with an inhibitor. This structure provides an unprecedented opportunity for structure-guided design of more potent and selective RabGGTase inhibitors.

Received: December 18, 2007
Published online: April 10, 2008

Keywords: inhibitors · prenylation · protein modifications · protein structures · transferases

[1] K. F. Leung, R. Baron, M. C. Seabra, *J. Lipid Res.* **2005**, *47*, 467 – 475.
[2] M. Miaczynska, S. Christoforidis, A. Giner, A. Shevchenko, S. Uttenweiler-Joseph, B. Habermann, M. Wilm, R. G. Parton, M. Zerial, *Cell* **2004**, *116*, 445 – 456, and references therein.
[3] P. J. Casey, M. C. Seabra, *J. Biol. Chem.* **1996**, *271*, 5289 – 5292.
[4] a) A. D. Hamilton, S. M. Sebti, *Oncogene* **2000**, *19*, 6584 – 6593; b) R. A. Gibbs, T. J. Zahn, J. S. Sebolt-Leopold, *Curr. Med. Chem.* **2001**, *8*, 1437 – 1465.
[5] F. E. Oualid, L. H. Cohen, G. A. van der Marel, M. Overhand, *Curr. Med. Chem.* **2006**, *13*, 2385 – 2427.
[6] F. P. Coxon, M. H. Helfrich, B. Larijani, M. Muzylak, J. E. Dunford, D. Marshall, A. D. McKinnon, S. A. Nesbitt, M. A. Horton, M. C. Seabra, F. H. Ebetino, M. J. Rogers, *J. Biol. Chem.* **2001**, *276*, 48213 – 48222. The IC_{50} value of the phosphonocarboxylate NE10790 was determined to be 502 ± 113 μM: see reference [11].
[7] M. R. Lackner, R. M. Kindt, P. M. Carroll, K. Brown, M. R. Cancilla, C. Chen, H. de Silva, Y. Franke, B. Guan, T. Heuer, T. Hung, K. Keegan, J. M. Lee, V. Manne, C. O'Brien, D. Parry, J. J. Perez-Villar, R. K. Reddy, H. Xiao, H. Zhan, M. Cockett, G. Plowman, K. Fitzgerald, M. Costa, P. Ross-Macdonald, *Cancer Cell* **2005**, *7*, 325 – 336. In this paper, nanomolar inhibitors of RabGGTase are described. However, they are even better inhibitors of FTase, that is, they are nonselective.
[8] P. A. Konstantinopoulos, M. V. Karamanzis, A. G. Papavassiliou, *Nat. Rev. Drug Discovery* **2007**, *6*, 541 – 555.
[9] a) K. Hinterding, P. Hagebuch, J. Retey, H. Waldmann, *Angew. Chem.* **1998**, *110*, 1298 – 1301; *Angew. Chem. Int. Ed.* **1998**, *37*, 1236 – 1239; b) M. Thutewohl, L. Kissau, B. Popkirova, I. M. Karagumi, T. Nowak, M. Bate, J. Kuhlmann, O. Müller, H. Waldmann, *Angew. Chem.* **2002**, *114*, 3768 – 3772; *Angew. Chem. Int. Ed.* **2002**, *41*, 3616 – 3620; c) M. Thutewohl, H. Waldmann, *Bioorg. Med. Chem.* **2003**, *11*, 2591 – 2615; d) M. Thutewohl, L. Kissau, B. Popkirova, I. M. Karagumi, T. Nowak, M. Bate, J. Kuhlmann, O. Müller, H. Waldmann, *Bioorg. Med. Chem.* **2003**, *11*, 2617 – 2626.
[10] B. Dursina, R. Reents, C. Delon, Y.-W. Wu, M. Kulharia, M. Thutewohl, A. Veligodsky, A. Kalinin, V. Evstifeev, D. Ciobanu, S. E. Szedlacsek, H. Waldmann, R. S. Goody, K. Alexandrov, *J. Am. Chem. Soc.* **2006**, *128*, 2822 – 2835.
[11] a) Y.-W. Wu, H. Waldmann, R. Reents, F. H. Ebetino, R. S. Goody, K. Alexandrov, *ChemBioChem* **2006**, *7*, 1859 – 1861; b) Y.-W. Wu, K. Alexandrov, L. Brunsveld, *Nat. Protocols* **2007**, *2*, 2704 – 2711.
[12] J. S. Taylor, T. S. Reid, K. L. Terry, P. J. Casey, L. S. Beese, *EMBO J.* **2003**, *22*, 5963 – 5974.
[13] While our data were in press different selective inhibitors of RabGGTase were reported: M. Watanabe, H. D. G. Fiji, L. Guo, L. Chan, S. S. Kinderman, D. J. Slamon, O. Kwon, F. Tamanoi, *J. Biol. Chem.*, in press, http://www.jbc.org/cgi/doi/10.1074/jbc.M706229200.

